

and surface albedo based on *Charlson et al.* [1991], we find large differences. If we assume the same forcing for the global and annual average, that is, $\mu_0=0.5$ and $R_s=0.114$ then our calculations result in a forcing which is up to a factor of 1.6 larger for large solar zenith angles and high surface albedos and substantially smaller for small zenith angles and low surface albedos. Especially if the focus is on the regional effects of sulfate changes, the more sophisticated fit (Eq.4.2) should be used.

Differences between computations of the radiative forcing using daily average parameters and integrating the diurnal cycle can occur because our analytical fit (Eq.4.2) is not proportional to μ_0 . The largest differences of up to 0.06 Wm^{-2} per 0.01 optical depth are found at low latitudes over oceans, where μ_0 varies most during daytime and the surface is relatively dark. When adopting daily averages, the computed radiative forcing is more negative or less positive than the forcing evaluated with the inclusion of the diurnal cycle.

4.6 Discussion

4.6.1 Ozone and Sulfate

The radiative forcing evaluated for tropospheric ozone and sulfate aerosols show characteristic patterns in space and time. Both components are formed downwind of industrial areas. However, there are several important differences. First, the shorter atmospheric residence time of sulfate (a few days) as compared to ozone (a few weeks) causes the pattern of sulfate forcing to show a larger variability. Second, the seasonal cycles of the concentration changes are different. The largest ozone increases occur in July, due to efficient photochemical processes, while the largest increase in modeled sulfate burden occurs in March, both over the industrial regions of the northern hemisphere. Third, the radiative forcings of both constituents have different dependencies on radiative parameters, which results in different patterns and seasonal cycles of the normalized forcing (i.e., forcing for fixed increases). The most important radiative parameters are surface temperature for the longwave forcing, surface albedo as well as solar zenith angle for the shortwave forcing, and cloudiness for the forcing in both the longwave and shortwave spectral region.

As the longwave forcing dominates for O_3 , a fixed and vertically uniform change (e.g., 10 DU) in the troposphere is associated with a decreasing forcing from equator to poles. Also, for the same hypothetical change, it is larger over relatively warm continents than over the cooler oceans in summer, while reversed in winter. The role of cloudiness is twofold: It masks the greenhouse effect of tropospheric O_3 but it enhances the shortwave effect. Due to these opposing effects the global and annual mean radiative forcing evaluated in a cloudy atmosphere is about 13% less than using clear sky situations, although, locally, large deviations can occur, because the ratio of longwave to shortwave forcing is highly variable.

The shortwave forcing of sulfate aerosol is critically dependent on the parameters μ_0 , f_d and R_s and therefore on latitude and season as well as on continental and marine conditions. For a

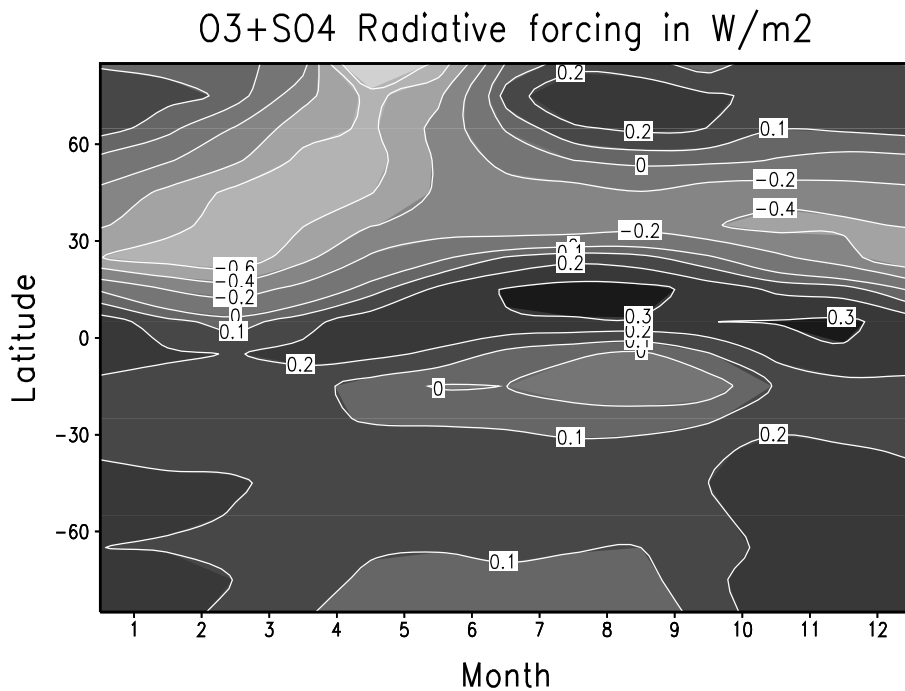


Figure 4.13: Hovmueller diagram of the zonal mean total radiative forcing (in Wm^{-2}) due to tropospheric ozone and sulfate changes for the period 1850-1990.

hypothetical globally uniform change of sulfate burden, the clear sky forcing would maximize somewhere at the midlatitudes, depending on surface albedo and season (day fraction). In contrast with O_3 , the shortwave radiative forcing by sulfate aerosols is reduced by clouds. Total cloud cover does not yield a zero forcing as suggested by *Charlson et al.* [1991]. We find a cloud factor, which is the ratio between the forcing calculated for average cloudiness and clear sky, of 0.75 (global and annual average changes 1850-1990) and about 0.82 for the same month over the period 1990-2050. The former value is somewhat higher than the cloud factor found by *Boucher and Anderson* [1995], 0.61, as a result of their larger average cloudiness of about 0.53 against 0.46 in this study. Nevertheless, our clear sky forcing of -0.49 Wm^{-2} is in close agreement with their value, -0.48 Wm^{-2} . The future scenario gives an even higher value caused by a shift of aerosol pollution toward less cloudy areas. Hence the cloud factor strongly depends on the pattern of sulfate change, and one may question the relevance of this parameter.

If we consider the seasonal cycle of the zonal mean radiative forcing by both tropospheric ozone and sulfate aerosol changes, over the industrial period (1850-1990), the region between 20°N and 55°N shows a negative forcing due to sulfate with a maximum occurring in March (Figure 4.13). The March maximum is a complex interplay between SO_x wintertime emissions

being relatively high, SO₂ oxidation becoming increasingly efficient, and radiation effects. The ozone forcing is dominant at high latitudes (>55°N) from June to February, with a maximum positive forcing of 0.3 Wm⁻² at 75°N in July. In contrast, very large negative values up to -1.3 Wm⁻² occur over the north polar region in April. Thus, at high latitudes the strongest seasonal cycle occurs. The southern hemisphere and the tropics show a small positive forcing, again due to ozone changes. An exception is the region around 15°S in the period May-September, when the sulfate effect apparently dominates the ozone effect, both produced by biomass burning. The net zonal and annual mean radiative forcing is negative northward of 20°N and reaches a minimum value of -0.44 Wm⁻² at 35°N.

In January the radiative forcing is negative over large parts of the northern hemispheric continents (Figure 4.14a). In fact, this illustrates the differences between ozone and sulfate dependencies on the various radiatively relevant parameters. Ozone forcing is relatively small in winter due to the low surface temperatures and insolation, whereas the sulfate effect can still be considerable due to the efficient backscatter to space for large solar zenith angles. A maximum negative forcing is found over the southeast Asia region (-3.7 Wm⁻²) and over the United States (-1.7 Wm⁻²). In July the total area of negative forcing over the northern hemispheric continents is much smaller than in winter (Figure 4.14b). The Greenland area has a strong positive forcing due to the fact that the ozone forcing is quite effective over areas with a high surface albedo, while the sulfate forcing is minimized. The seasonality of the forcing is reinforced by the fact that in the northern hemisphere ozone changes are about 15% higher and sulfate changes are about 30% lower in July as compared to January. The situation in the southern hemisphere, mainly over southern Africa and South America, is reversed.

In order to illustrate the sensitivities for ozone (longwave and shortwave), as well as for sulfate aerosols (shortwave), we have tabulated these values, that is, the changes over the period 1850-1990 and the consequent total radiative forcing (clear sky and cloudy sky) for January and July at three locations and for the northern hemisphere (Table 4.3). The locations selected are in Europe (55°N, 15°E), in the United States (35°N, 275°E) and in southeast Asia (25°N, 115°E), where the forcing is considerable and reaches a maximum in some cases. For high latitudes (e.g., 55°N) the (clear sky) sensitivity of sulfate is much smaller in winter than in summer, while for lower latitudes (e.g., 25°N) the situation is reversed. For the United States location at 35°N the clear sky sensitivity is the same in January and July. This is also the case for the northern hemispheric mean sensitivity. Sulfate forcing is about 20% less effective over continental areas compared to the oceans, because of the low surface albedos. Most of the sulfate change, about 75% in January and 85% in July, occurs over land as a result of the short residence time. In contrast, ozone changes are much more zonally dispersed, because the residence time of ozone is larger. In July, about 60% of the ozone change occurs over land as the largest production occurs over Europe, while the Eurasian continent is affected downwind. The longwave sensitivity of ozone for the three selected locations is a factor 1.5 larger in July as compared to January due to the higher continental surface temperatures. Over oceans this difference is considerably smaller.

4. Radiative Forcing due to Tropospheric Ozone and Sulfate Aerosols

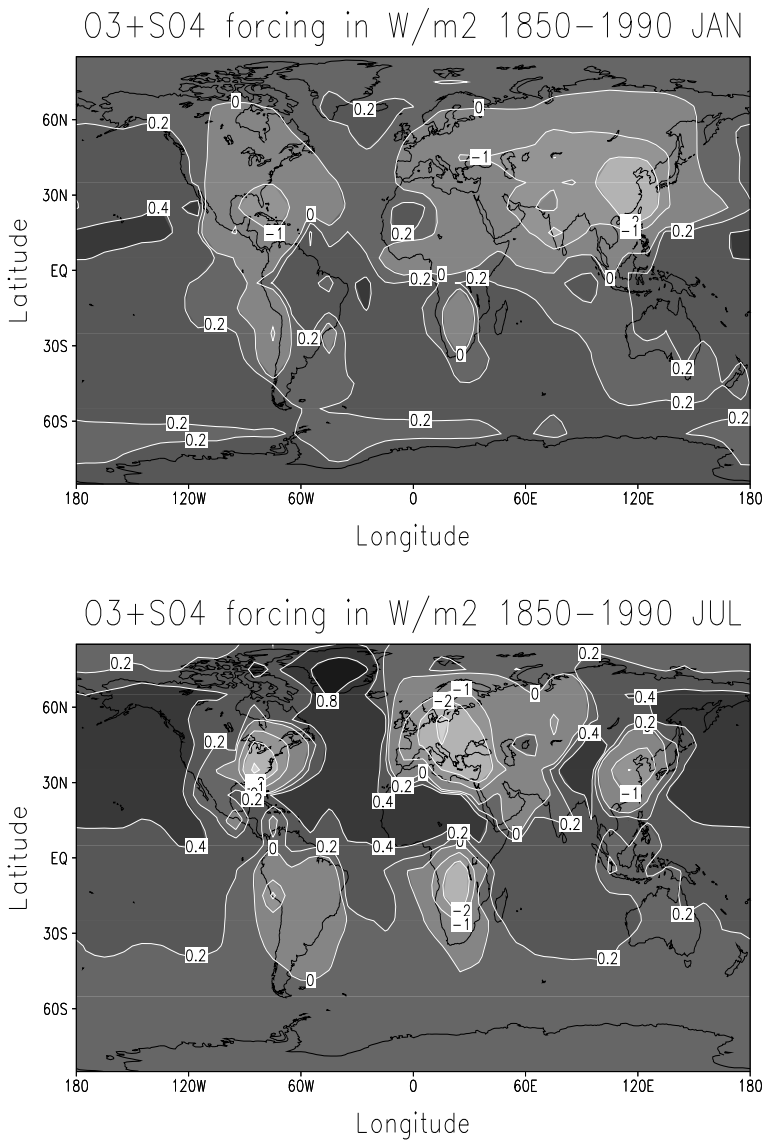


Figure 4.14: (a) January average total radiative forcing (in Wm^{-2}) due to tropospheric ozone and sulfate changes for the period 1850-1990. (b) July average total radiative forcing (in Wm^{-2}) due to tropospheric ozone and sulfate changes for the period 1850-1990.

The difference of the O_3 shortwave sensitivity between January and July is predominantly dependent on the amount of insolation. Hence, high latitudes show a stronger seasonal cycle than low latitudes. Averaged over the northern hemisphere, there is a factor of about 2 difference.

4. Radiative Forcing due to Tropospheric Ozone and Sulfate Aerosols

Table 4.3: January and July Clear sky and Average Cloudiness Sensitivities of Ozone and Sulfate Aerosol and Consequent Radiative Forcing for the Industrial Period 1850-1990. Here $\gamma_{LW,clr}$, $\gamma_{SW,clr}$, and $\gamma_{TOT,clr}$ are the longwave, shortwave, and total clear sky sensitivities, respectively. $\gamma_{TOT,clد}$ is the total sensitivity under average cloudiness conditions (for ozone per 10 DU and for sulfate per 0.01 optical depth). Also shown are the calculated O_3 and SO_4 changes and total radiative forcing (ΔF_{clr} is clear sky forcing, and $\Delta F_{clد}$ is forcing for average cloudiness). OD denotes optical depth.

	Month	Location			Northern Hemisphere		
		Europe	United States	southeast Asia	Mean	Ocean	Land
Cloud cover, %	Jan.	62	49	59	43	45	40
	July	42	37	53	45	50	41
<i>Ozone</i>							
$\gamma_{LW,clr}$, $W m^{-2}/10$ DU	Jan.	0.27	0.27	0.34	0.39	0.46	0.37
	July	0.42	0.45	0.51	0.51	0.54	0.48
$\gamma_{SW,clr}$, $W m^{-2}/10$ DU	Jan.	0.03	0.06	0.06	0.05	0.04	0.05
	July	0.09	0.10	0.08	0.09	0.07	0.10
$\gamma_{TOT,clr}$, $W m^{-2}/10$ DU	Jan.	0.30	0.33	0.40	0.43	0.51	0.37
	July	0.51	0.55	0.59	0.59	0.61	0.58
$\gamma_{TOT,clد}$, $W m^{-2}/10$ DU	Jan.	0.27	0.30	0.33	0.37	0.42	0.33
	July	0.45	0.46	0.47	0.53	0.53	0.52
ΔO_3 , DU	Jan.	10.9	11.7	12.4	10.1	9.5	10.7
	July	19.2	18.3	11.8	11.6	9.7	13.5
<i>Sulfate</i>							
$\gamma_{SW,clr}$, $W m^{-2}/0.01$ OD	Jan.	-0.20	-0.24	-0.26	-0.22	-0.25	-0.20
	July	-0.38	-0.24	-0.21	-0.23	-0.27	-0.23
$\gamma_{SW,clد}$, $W m^{-2}/0.01$ OD	Jan.	-0.10	-0.12	-0.15	-0.16	-0.17	-0.15
	July	-0.32	-0.22	-0.17	-0.19	-0.18	-0.19
ΔSO_4 , 0.01 OD	Jan.	10.8	9.7	27.4	4.2	2.3	6.1
	July	17.6	25.7	9.2	3.0	0.8	5.0
<i>Ozone+Sulfate</i>							
ΔF_{clr} , $W m^{-2}$	Jan.	-1.82	-1.91	-6.64	-0.45	-0.07	-0.82
	July	-5.60	-5.15	-1.17	0.03	0.39	-0.31
$\Delta F_{clد}$, $W m^{-2}$	Jan.	-0.77	-0.78	-3.74	-0.26	0.02	-0.54
	July	-4.59	-4.61	-0.96	0.07	0.38	-0.22

The reduction of the radiative forcing in the presence of clouds is larger for sulfate than for ozone. Also, clouds are more effective in reducing the forcing of sulfate in winter compared to the summer season, with 27% in January and 18% in July (northern hemispheric mean, see Table 4.3). For ozone the cloud reduction percentages are 14% and 12%, respectively.

4.6.2 Changes of the Radiation Balance for 1850-1990

The radiative forcing due to increases of the well-mixed greenhouse gases (CO_2 , CH_4 , N_2O , and CFCs) over the industrial period, which occurs predominantly in the longwave spectral range, is dependent on latitude, season, and continental and maritime conditions, mainly due to temperature differences between surface and tropopause. Also, atmospheric residence times of these gases are decades to more than a century, resulting in hemispheric symmetry. The zonal mean forcing thus ranges from about 1.2 Wm^{-2} over high latitudes in the winter season to 2.6 Wm^{-2} in the tropical regions. This implies that the current combined zonal mean forcing due to the well-mixed greenhouse gases, tropospheric ozone, and sulfate is positive (Figure 4.15). The lowest zonal mean forcing with values less than 1 Wm^{-2} occurs in March and April northward of about 50°N . However, since sulfate changes are quite localized over the industrial regions and over areas where biomass burning is taking place, some spots of negative radiative forcing occur, which can exceed the positive forcing due to the well-mixed greenhouse gases and tropospheric ozone. In January, such a spot is located over the southeast Asian region, where values of the total radiative forcing up to -2 Wm^{-2} are found. Surprisingly, four spots of negative forcing, over Europe, the United States, southeast Asia and central Africa, occur in July, but these are surrounded by large areas (most parts of the continents and all oceans) with a relatively strong positive forcing. Hence, during all seasons, regions of negative forcing show up, while in July the largest longitudinal gradients occur. Although ammonium nitrate is incorporated in these computations, the spots of negative total forcing still appear without these aerosols over the same regions, except perhaps over the southeast Asian region in July.

4.7 Conclusion

The radiative forcing of tropospheric ozone and sulfate changes since preindustrial times, as well as for the future, based on the IS92a emission scenario [IPCC, 1992], has been assessed using a wideband radiation scheme. Both short-lived atmospheric constituents are highly variable in space and time, and so are their changes. Therefore, we have adopted the three-dimensional fields of temperature, water vapor (prescribed Oort [1983] data), and the considered atmospheric constituents, computed with the MOGUNTIA transportchemistry model. In order to get reliable estimates of the radiative forcing, we have included the climatology of surface albedo and cloud cover, as well as a stratospheric ozone distribution and a latitudinally dependent tropopause height.

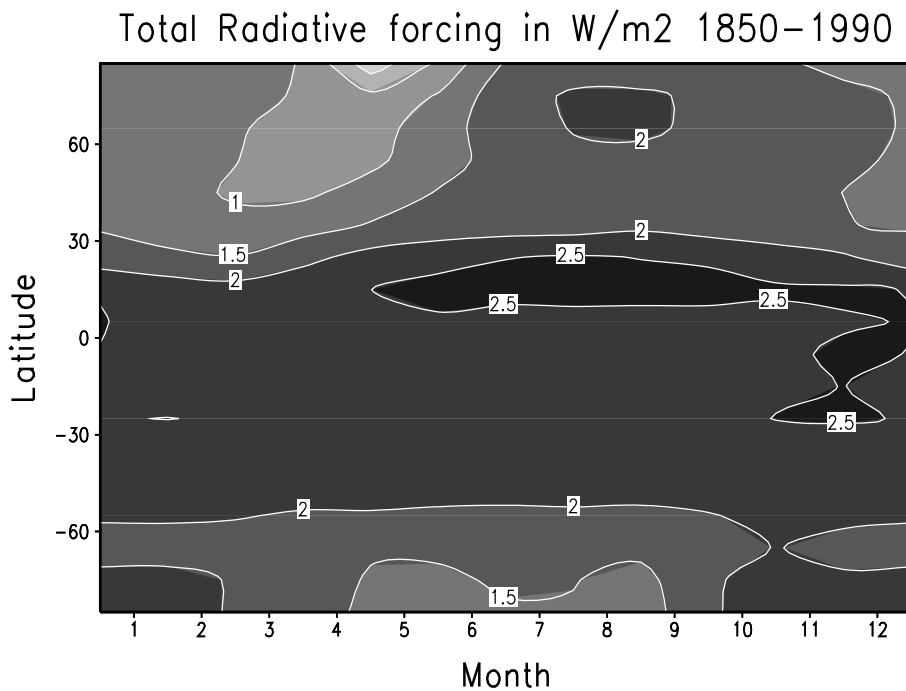


Figure 4.15: Hovmueller diagram of the zonal mean total radiative forcing (in Wm^{-2}) due to the well-mixed greenhouse gases, tropospheric ozone and sulfate changes for the period 1850-1990.

We calculate a globally and annually averaged radiative forcing of $0.38 \pm 0.15 \text{ Wm}^{-2}$ due to a column O_3 increase of about 8 DU in the troposphere since preindustrial times. Ozone changes are at maximum downwind of the industrialized regions and biomass burning areas. This implies some asymmetry between both hemispheres. Peak values of about 1 Wm^{-2} are found over northern Africa and Saudi Arabia. The uncertainty has been estimated from the examined sensitivity of the ozone forcing and a radiation code intercomparison [Shine *et al.*, 1995]. In addition, significant uncertainty is associated with the chemistry-transport modeling, in particular of ozone changes in the upper troposphere [Dentener *et al.*, 1995]. This region is most sensitive for ozone changes as the contrast between local temperature and surface temperature is largest. Previous studies reported somewhat higher global average radiative forcings, but differences can be explained in terms of ozone sensitivity and of the adopted concept of radiative forcing.

For the industrial period we examined the role of the changed sulfate burden in the atmosphere and found a globally and annually averaged radiative forcing of -0.36 Wm^{-2} , which is somewhat higher in an absolute sense than in a recent study [Boucher and Anderson, 1995]. This can be attributed to differences in imposed cloud fields, as our clear sky forcing is in close agreement. If we take the large uncertainty ranges into consideration, our result is comparable

to all earlier studies, except perhaps with that of *Taylor and Penner* [1994], who found a rather large global mean forcing of -0.9 Wm^{-2} . Sulfate aerosol increases are to a larger degree confined to the industrial areas in the northern hemisphere and to biomass burning regions in Africa and South America than of ozone increases, due to the shorter atmospheric residence time (a few days versus a few weeks). This results in a larger variability in space and time with peak values up to -5.5 Wm^{-2} over Europe and the United States in July, and -4 Wm^{-2} over southeast Asia in January.

The effect of relative humidity on the aerosol optical parameters, and thus on the sulfate forcing, has been studied for the given distribution of change. It appears that globally and annually averaged differences between the forcing computed with fixed relative humidity and that with a dependence is quite small, -0.32 Wm^{-2} against -0.36 Wm^{-2} . Zonal averages show larger differences up to 0.2 Wm^{-2} , especially in the dry subtropics and the humid mid-latitudes. Regionally, differences up to 5 Wm^{-2} are found. Hence, if the focus is on regional forcing, relative humidity effects should be included.

We also examined the role of ammonium nitrate in perturbing the radiation balance. Averaged over the globe its forcing is an order of magnitude smaller than that of sulfate. However, peak values of -0.8 Wm^{-2} over western Europe are found in July. Although measurements in the Netherlands confirm the significance of nitrate in summer, these results should be handled with caution as the relevance for other areas is not established.

On a global scale, the sulfate annual mean forcing approximately balances that of ozone. However, large regional differences occur due to three effects. First, the pattern of sulfate forcing shows a higher variability compared to ozone. Second, the seasonal cycle is different, showing the largest ozone increases in July due to efficient photochemical processes and the largest increase in sulfate burden in March in the northern hemisphere. Third, the radiative forcings of both constituents depend differently on the radiative parameters, resulting in different patterns and seasonal cycles. We find that the combined effects imply a net negative radiative forcing in the winter season in the northern hemisphere and a net positive forcing during summer.

Part of this study is devoted to evaluation of the forcing sensitivities of ozone and sulfate. Ozone is active in the longwave and shortwave spectral region (on average, the longwave forcing is about 80% of the total), whereas sulfate aerosols are mainly active in the shortwave region. As a consequence, the ozone forcing maximizes over areas with high surface temperatures and for changes in the vicinity of the tropopause, occurring in summer and over regions with a large convective activity. Clouds mask the greenhouse effect of tropospheric ozone, but enhance the shortwave forcing. The net effect is a decrease of about 13% for the global and annual mean. Furthermore, the normalized shortwave forcing is linearly dependent on the product of surface albedo and μ_0 . Hence, the ratio of longwave to shortwave forcing is smallest over cold, bright surfaces and in case of large insolation, for example, over Antarctica in January. The dependency of the shortwave forcing of sulfate aerosol on surface albedo and angle of insolation is quite different from that of ozone. A maximum normalized forcing is found for average solar zenith

angles during daytime at midlatitudes due to the competition between the amount of insolation and changes in the amount of backscattered radiation.

We developed analytical fits for both the ozone and sulfate shortwave forcings, in which we included the most relevant parameters as mentioned above. These parameterizations have been tested using a sophisticated radiation model for a wide range of situations. We demonstrate that our analytical expression for the quantification of the sulfate forcing matches the radiation computations much better than the commonly used (1-surface albedo)² relationship [Charlson *et al.*, 1991]. It also accounts for conditions of high surface albedos in combination with sufficiently small solar zenith angles, when the sulfate forcing can be positive. This can occur, for example, over Antarctica in January and over Greenland in July. Furthermore, clouds efficiently reduce the sulfate forcing. We find cloud reduction factors of 0.75 and 0.82 for increases over the period 1850-1990 and 1990-2050, respectively. Also, large seasonal differences are found, indicating that the distribution of clouds and sulfate changes determines this factor. Therefore, the relevance of this parameter is limited.

We also examined the possible tropospheric ozone and sulfate changes and the consequent forcings toward 2050. The expected ozone increase for the next half century is about 70% of the change since preindustrial times, and so is the computed forcing, which is 0.28 Wm^{-2} globally and annually averaged. It is interesting to note that the regions of maximum ozone change are shifting southward as compared to the 1850-1990 period due to enhanced industrial activities in central America and in southern Asia. Here, peak values of 0.9 Wm^{-2} are expected. Related to this southward shift, the maximum ozone forcing is expected to occur in August instead of July, when conditions are optimal for the photochemical processes as well as for the longwave forcing component. In contrast with the reduced O_3 trend over the period 1990-2050, as compared to the period 1850-1990, sulfate changes are expected to increase in the future, resulting in a global average radiative forcing of -0.59 Wm^{-2} . Northern hemispheric changes increase by about 13% and in the southern hemisphere the sulfate burden may be more than doubled compared to the 1850-1990 change. The India and southeast Asian regions are expected to contribute most, with a peak value of -19 Wm^{-2} . Similar to the O_3 changes, we expect a southward shift of the sulfate burden associated with increasing industrial activities by countries with emerging activities in the near future.

As compared to the current radiative forcing due to the well-mixed greenhouse gases, tropospheric ozone increases contribute about 15%. In 2050 the contribution of ozone to the total positive forcing since preindustrial times is expected to be somewhat smaller, but still significant. Increases of the sulfate burden act to (over)compensate the positive forcing on a regional scale. In January this is the case over large parts of southeast Asia, while in July four spots over the industrialized regions and over central Africa can be distinguished. In this month the gradients of total radiative forcing in the northern hemisphere are largest. Globally averaged, the greenhouse gases, including tropospheric ozone, maintain a dominant role.

acknowledgments We thank Ingrid Schult for kindly providing us the aerosol optical parameters. The 2050 sulfur emission was made available by Henning Rodhe. We acknowledge Piet Stammes and Bert Holtlag for their help in evaluating this paper. Also, we would like to thank the SINDICATE group and in particular Yves Balkanski, Lennart Bengtsson, Paul Crutzen, Hans Feichter, Maria Kanakidou, Frank Raes, and Erich Roeckner, for their keen interest and many valuable discussions. This study was part of the SINDICATE project, supported by the Environmental Program of the European Union (DG-XII).